OPEN

Citation: Cell Death and Disease (2014) 5, e1081; doi:10.1038/cddis.2014.42

www.nature.com/cddis

MYCN gene expression is required for the onset of the differentiation programme in neuroblastoma cells

L Guglielmi[1,3], C Cinnella[1,3], M Nardella[1], G Maresca[1], A Valentini[2], D Mercanti[1], A Felsani[1] and I D'Agnano*[,1]

Neuroblastoma is an embryonic tumour of the sympathetic nervous system and is one of the most common cancers in childhood. A high differentiation stage has been associated with a favourable outcome; however, the mechanisms governing neuroblastoma cell differentiation are not completely understood. The *MYCN* gene is considered the hallmark of neuroblastoma. Even though it has been reported that *MYCN* has a role during embryonic development, it is needed its decrease so that differentiation can be completed. We aimed to better define the role of *MYCN* in the differentiation processes, particularly during the early stages. Considering the ability of *MYCN* to regulate non-coding RNAs, our hypothesis was that N-Myc protein might be necessary to activate differentiation (mimicking embryonic development events) by regulating miRNAs critical for this process. We show that *MYCN* expression increased in embryonic cortical neural precursor cells at an early stage after differentiation induction. To investigate our hypothesis, we used human neuroblastoma cell lines. In LAN-5 neuroblastoma cells, *MYCN* was upregulated after 2 days of differentiation induction before its expected downregulation. Positive modulation of various differentiation markers was associated with the increased *MYCN* expression. Similarly, *MYCN* silencing inhibited such differentiation, leading to negative modulation of various differentiation markers. Furthermore, *MYCN* gene overexpression in the poorly differentiating neuroblastoma cell line SK-N-AS restored the ability of such cells to differentiate. We identified three key miRNAs, which could regulate the onset of differentiation programme in the neuroblastoma cells in which we modulated *MYCN*. Interestingly, these effects were accompanied by changes in the apoptotic compartment evaluated both as expression of apoptosis-related genes and as fraction of apoptotic cells. Therefore, our idea is that *MYCN* is necessary during the activation of neuroblastoma differentiation to induce apoptosis in cells that are not committed to differentiate.
Cell Death and Disease (2014) **5,** e1081; doi:10.1038/cddis.2014.42; published online 20 February 2014
Subject Category: Cancer

Neuroblastoma is an embryonic tumour of the sympathetic nervous system and is one of the most common childhood cancers. The clinical signs and symptoms of neuroblastoma are extremely variable.[1] A high differentiation stage has been associated with a favourable outcome;[1] however, the mechanisms governing neuroblastoma cell differentiation are not completely understood. Nevertheless, the ability of many neuroblastoma cell lines to maintain their differentiation capability *in vitro* has made them suitable models for studying human neuronal differentiation.[2]

It is well known that the *MYC* family member N-Myc, encoded by *MYCN*, has a key role during neuroblastoma differentiation. N-Myc has been found to be overexpressed in approximately 25% of primary neuroblastoma tumours.[3] The *MYC* gene family is composed of three members, *MYC*, *MYCN* and *MYCL*. The Myc proteins act as transcription factors: they recognise a consensus sequence (CACGTG) known as the E-box sequence and form a heterodimeric complex with their functional partner, Max. The Myc-Max heterodimer recruits other transcriptional co-factors and activates or represses gene expression.[4,5] Similar to the other Myc proteins, N-Myc is a transcription factor that controls the expression of many target genes involved in fundamental cellular processes.[6,7] c-Myc was found to be overexpressed in Burkitt lymphomas; however, during mouse embryogenesis and in highly proliferative adult tissues it is usually expressed, functioning as an inhibitor of differentiation processes and a promoter of cell proliferation.[8] Interestingly, *MYCN* shows a more targeted expression pattern, with temporal and tissue specificity. It is first detected during the seventh day of pregnancy, is observed at high levels during the ninth and eleventh days and rapidly decreases after the twelfth day.[9,10] The importance of *MYCN* expression during the first steps of developmental processes is demonstrated by mutations in the human *MYCN* gene being associated with birth defects. Mouse embryos defective for *MYCN* are unable to survive past embryonic stage E11.5 and exhibit hypoplasia in diverse organs and tissues: strongly reduced thickness of the encephalic walls, reduction of mature neurons in the ganglia of the trunk region, hearts underdeveloped often retaining the S-shape typical of 9-day-old embryos, marked underdevelopment in the lung airway epithelium, failure in the organisation of the mesonephros of the genitourinary system, absence of a bulging stomach structures.[11–16] Moreover, in

[1]CNR, Institute of Cell Biology and Neurobiology, Rome, Italy and [2]PTV, Laboratory Medicine and Internal Medicine Departments, University of Rome 'Tor Vergata', Rome, Italy
*Corresponding author: I D'Agnano, CNR, Institute of Cell Biology and Neurobiology, Via Ramarini 32, 00015 Monterotondo, Roma, Italy. Tel: +39 6 90091341; Fax: +390 6 90091260; E-mail: igea.dagnano@cnr.it
[3]These authors contributed equally to this work.
Keywords: *MYCN*; neuroblastoma; differentiation; miRNA
Abbreviations: RA, retinoic acid; NF200, neurofilament 200; BrdU, bromodeoxyuridine; PI, propidium iodide; qRT-PCR, quantitative PCR
Received 23.7.13; revised 09.1.14; accepted 13.1.14; Edited by G Melino

adult tissues, *MYCN* is expressed at early stages in developing B cells and at low levels in the brain, testis and heart.[17,18] Nevertheless, it is widely accepted that *MYCN* expression undergoes a necessary decrease during differentiation processes; otherwise, high *MYCN* levels lead to a neoplastic phenotype.[19]

The aim of this work was to study the role of the N-Myc protein in neuroblastoma differentiation processes, particularly during the early stages. Our hypothesis was that N-Myc might be necessary to activate neuroblastoma differentiation (mimicking embryonic development events) by regulating certain non-coding RNAs critical for differentiation.

Indeed, our data demonstrate that *MYCN* gene expression is required for neuroblastoma cells to activate the differentiation programme in the early stages. We found that N-Myc expression increased during the early differentiation phases, and its downregulation prevented differentiation in human neuroblastoma LAN-5 cells. Moreover, *MYCN* gene overexpression in the poorly differentiating neuroblastoma cell line SK-N-AS predisposed the cells to complete the differentiation process. These effects were accompanied by modulation of the apoptotic programme and were mediated by non-coding RNAs, which in turn regulated the expression of various apoptosis-related genes.

Results

Retinoic acid (RA) triggers differentiation in the human neuroblastoma LAN-5 cell line. First, we performed a comparative western blot analysis of the main proteins studied in the three cell models discussed in the paper (Supplementary Figure S1).

Figure 1a shows neurite outgrowth in LAN-5 cells cultured in a medium supplemented with 10 μM RA. Untreated cells continued expansion without changing morphology or shape; however, in RA-treated cells, neurite appeared after the first day of treatment and increased in number and length after 5 days. Moreover, neurite interconnections were stimulated by RA: the exposure caused the cells to form new networks. The expression of the differentiation marker neurofilament 200 (NF200) was induced by RA (Figure 1b).

Analysis of a group of typical molecular neuronal markers confirmed that RA treatment activated the differentiation programme in LAN-5 cells. Quantitative PCR (qRT-PCR) revealed increasing levels of *GAP43*, *ChAT*, *MAPT*, *SLC18A*, *ENO2* and *CDK5* (Figure 1c); western blotting analysis of GAP43 and ChAT proteins confirmed the qRT-PCR data (Figure 1d).

Differentiation induction was offset by a reduction in the growth of RA-treated cells; the mean doubling time was approximately 27 h in control cells and 54 h in RA-treated ones (Supplementary Figure S2a). RA prevented cell growth by arresting cells in the G0/G1 phase of the cell cycle (the percentage of cells in G0/G1 was 50.40% in control cells and 71.48% in RA-treated cells after 3 days of growth; Supplementary Figure S2b). Moreover, a bromodeoxyuridine (BrdU) incorporation assay revealed reduced DNA synthesis after RA exposure. The percentage of cells incorporating BrdU was 53% for untreated control cells and 21% for RA-treated cells (Supplementary Figure S2c). Consistent with the increase in the percentage of cells in the G0/G1 cell cycle phase, cyclin A was downregulated, and the kinase inhibitor $p27^{kip1}$ was upregulated (Supplementary Figure S2d).

N-Myc expression increases during the early phases of RA-induced differentiation in cells of neural origin. LAN-5 cells showed an increase in N-Myc protein when exposed to RA. The maximal N-Myc expression was evident between the first and the third day of treatment (Figure 2a). Afterwards, N-Myc expression levels started to decrease. Analysis of *MYCN* levels using qRT-PCR confirmed the results observed by western blot analysis, revealing a maximum of an approximately threefold enrichment of its mRNA during the early induction of differentiation (Figure 2b). We also examined the mRNA levels of a well-known downregulated downstream target of N-Myc, N-Myc downstream-regulated gene 1 (*NDRG1*),[20] to verify the functional implications of *MYCN* upregulation. As expected, qRT-PCR analysis revealed that the modulation of the N-Myc target *NDRG1* inversely paralleled *MYCN* modulation during differentiation (Figure 2b). The analysis of the sub-G1 fraction, indicative of apoptosis, during the RA-induced differentiation in LAN-5 cells revealed a peak in the sub-G1 region between the third and the fourth day of differentiation, when N-Myc expression was maximal (Figure 2c).

The *MYCN* expression analysis conducted in mouse cortical embryonic neural progenitor cells induced to differentiate revealed that the *MYCN* levels in these cells tracked those observed in LAN-5 cells during differentiation (Figure 2d). Evidently, *MYCN* expression increased during the early phases of differentiation and then decreased as expected. The observed increase in *CDK5* expression was consistent with the activation of differentiation. Interestingly, a significant decrease in *MYC* expression was observed from the early phases of differentiation, further supporting the idea that the *MYC* and *MYCN* genes might have different roles in the differentiation programme.

N-Myc is necessary to activate the differentiation programme in LAN-5 neuroblastoma cells. To determine whether and to what extent *MYCN* has a determining role in early differentiation, we silenced its expression in *MYCN*-amplified LAN-5 cells. We introduced an artificial miRNA to interfere with N-Myc expression. We evaluated N-Myc levels after downregulation, comparing Mock cells and *MYCN*-KD ones during RA treatment for 4 days (Figure 3a). We obtained a decrease in protein levels of approximately 70%, maintained at similar level during RA-induced differentiation. The downregulation of the *MYCN* transcripts was approximately 40%, and the levels of the N-Myc downstream target *NDRG1* were significantly upregulated (Figure 3b).

Phase contrast microscopy revealed a strong reduction of neurite formation in *MYCN*-KD cells even after RA treatment. In contrast, Mock cells continued to present neurite extensions (Figure 3c). In the same differentiation conditions in *MYCN*-KD cells, we did not observe any significant expression of the neurite marker NF200 (Figure 3d).

We studied plasma membrane polarisation using flow cytometry and fluorescent dyes responsive to acute changes in the plasma membrane potential to determine functional effects of *MYCN* downregulation in LAN-5 cells. As expected,

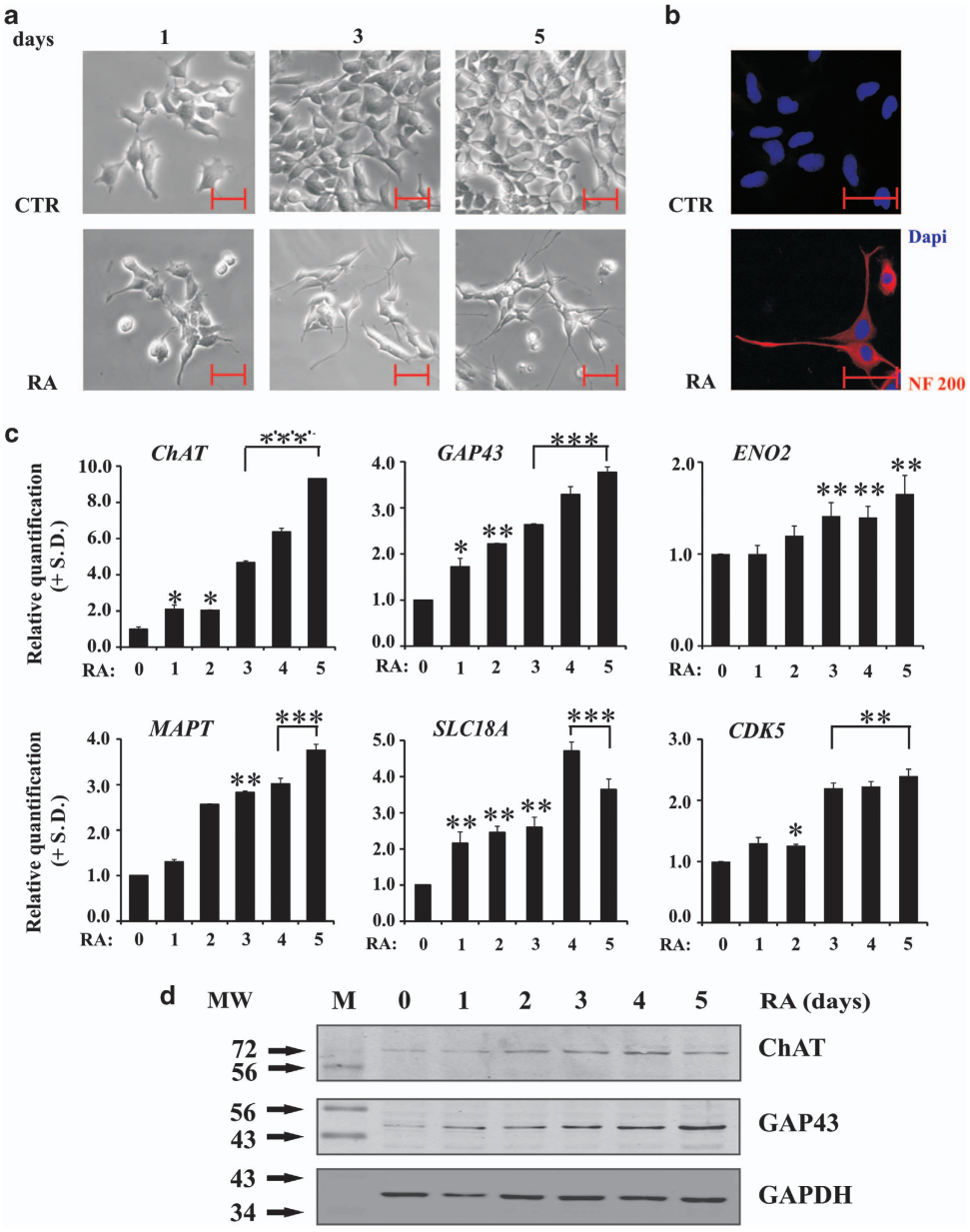

Figure 1 LAN-5 cells differentiate upon RA stimulus. (**a**) Inverted light microscope images of LAN-5 cells untreated (CTR) or RA treated for 1, 3 and 5 days. Scale bar, 50 μm. (**b**) Representative fluorescent images of LAN-5 cells untreated (CTR) or RA treated for 5 days. Red, NF200 immunostaining; blue, DAPI. Scale bar, 50 μm. (**c**) The levels of the indicated mRNA in LAN-5 cells untreated (0) or RA treated for 1, 2, 3, 4 and 5 days. The data are reported as the level of mRNA relative to the respective untreated cells and are the mean + S.D. ($n = 3$). Statistical significance, $^{*}P \leq 0.05$; $^{**}P \leq 0.01$; $^{***}P \leq 0.001$. (**d**) Representative blots of the indicated proteins in LAN-5 cells untreated (0) or RA treated for 1, 2, 3, 4 and 5 days. GAPDH expression was used to normalise protein loading. The experiment was repeated three times with similar results. M, molecular weight markers; MW, molecular weight

MYCN-KD cells were characterised by a reduced ability to polarise the plasma membrane compared with Mock cells. (Figure 4a). In addition, the membrane hyperpolarisation usually observed in RA-differentiated cells was prevented when the *MYCN* gene was downregulated (Figure 4b). We evaluated cell death in Mock and *MYCN*-KD cells by assessing the mitochondrial membrane potential. We found that the *MYCN*-silenced cells did not show any cell death after RA treatment, whereas the control Mock cells exposed to RA exhibited apoptosis (Figure 4c), suggesting that *MYCN* might be necessary in the early phases of differentiation to induce apoptosis in cells not committed to differentiation.

The expression of the molecular neuronal markers previously analysed in the differentiating LAN-5 cells was also studied after *MYCN* silencing. We observed inhibited expression levels of all four markers analysed at day 3 after RA treatment (Figure 4d).

N-Myc overexpression induces differentiation in poorly differentiating neuroblastoma cells. The SK-N-AS

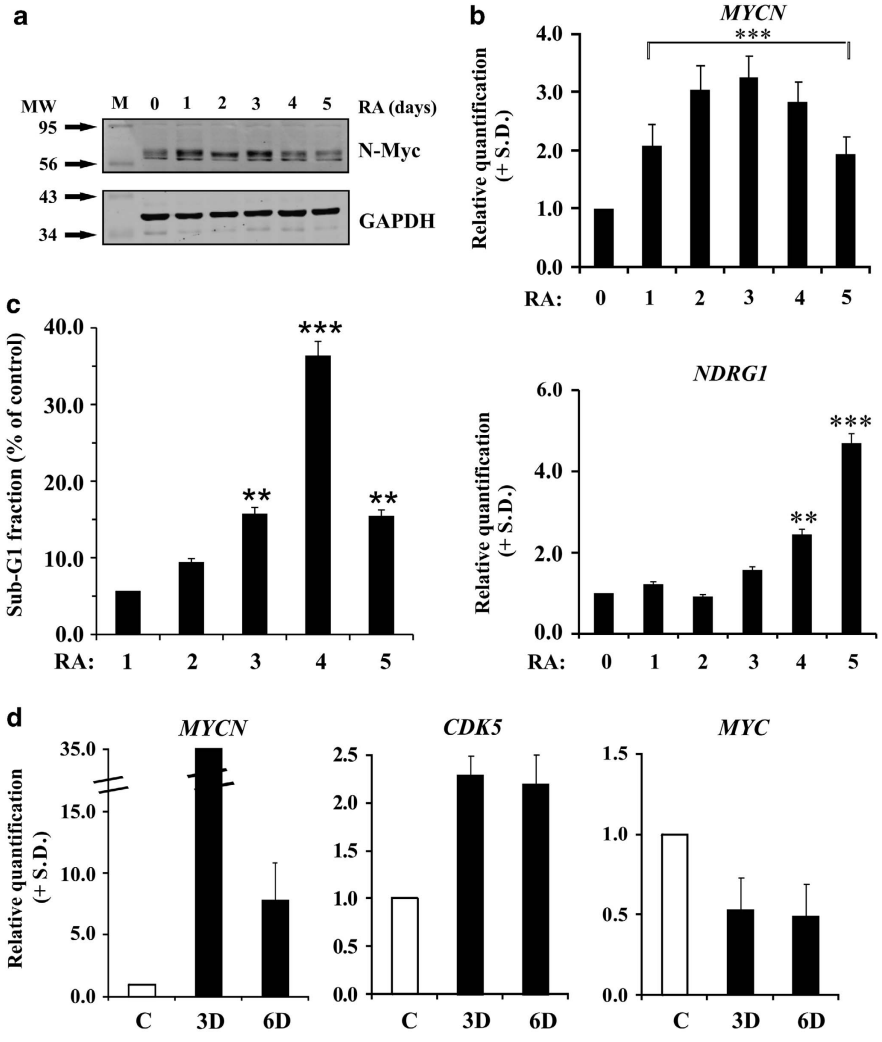

Figure 2 *MYCN* increases during the first days of differentiation in LAN-5 cells and in mouse cortical embryonic neural progenitors. (**a**) Representative blots of the N-Myc protein in LAN-5 cells untreated (0) or RA treated for 1, 2, 3, 4 and 5 days. GAPDH expression was used to normalise protein loading. The experiment was repeated three times showing similar results. M, molecular weight markers; MW, molecular weight. (**b**) Levels of the indicated mRNA in LAN-5 cells untreated (0) or RA treated for 1, 2, 3, 4 and 5 days. The data are reported as the level of mRNA relative to the respective untreated cells and are the mean + S.D. ($n = 3$). Statistical significance, $^{**}P \leq 0.01$; $^{***}P \leq 0.001$. (**c**) Sub-G1 fractions estimated on the DNA content histograms in LAN-5 cells treated with RA for 1, 2, 3, 4 and 5 days. Data are reported as percent of control. Statistical significance, $^{**}P \leq 0.01$; $^{***}P \leq 0.001$. (**d**) The levels of the indicated mRNA in mouse cortical embryonic neural progenitor cells undifferentiated (white) or induced to differentiate for 3 and 6 days (black). The data are reported as the level of mRNA relative to the respective untreated cells and are the mean + S.D. ($n = 3$). Statistical significance, $^{**}P \leq 0.01$; $^{***}P \leq 0.001$

neuroblastoma cell line shows a very poor capacity to differentiate after stimulation with RA, and these cells have a single copy of the *MYCN* gene, thus showing no overexpression of this gene.[21] We overexpressed the *MYCN* gene in these cells (Figure 5a) and studied differentiation activation after RA induction. The overexpression of the *MYCN* gene was also confirmed by the protein level (Figure 5b). Figure 5c shows the micrographs of SK-N-AS Mock and SK-N-AS *MYCN*+ cells, untreated or treated with RA for 3 days. In the presence of the *MYCN* gene, RA activated differentiation in SK-N-AS cells, as indicated by the neurite outgrowth, with most of them showing a bipolar shape. The number of cells with neurites increased by approximately 90% in *MYCN*+ cells after RA treatment. The neurite length was significantly increased in *MYCN*+ cells (Figure 5d; Mock cells, mean = 121 μm, median = 120 μm, range = 60–254 μm; *MYCN*+ cells, mean = 213 μm, median = 208 μm, range = 115–375 μm). NF200 immunostaining confirmed the ability of SK-N-AS *MYCN*+ cells to differentiate; NF200 was clearly expressed in these cells after RA exposure (Figure 5e). The analysis of *GAP43*, *CDK5* and *ENO2* differentiation marker genes corroborated that *MYCN* overexpression in SK-N-AS cells rendered these cells prone to differentiation after RA exposure (Figure 5f).

***MYCN* modulation modifies the expression of miRNAs involved in apoptosis preceding neuronal differentiation.** The analysis of specific miRNAs selected by *in silico* analysis (miRWalk[22]) and reported to be regulated by *MYCN* and at the same time involved in apoptosis and neuron

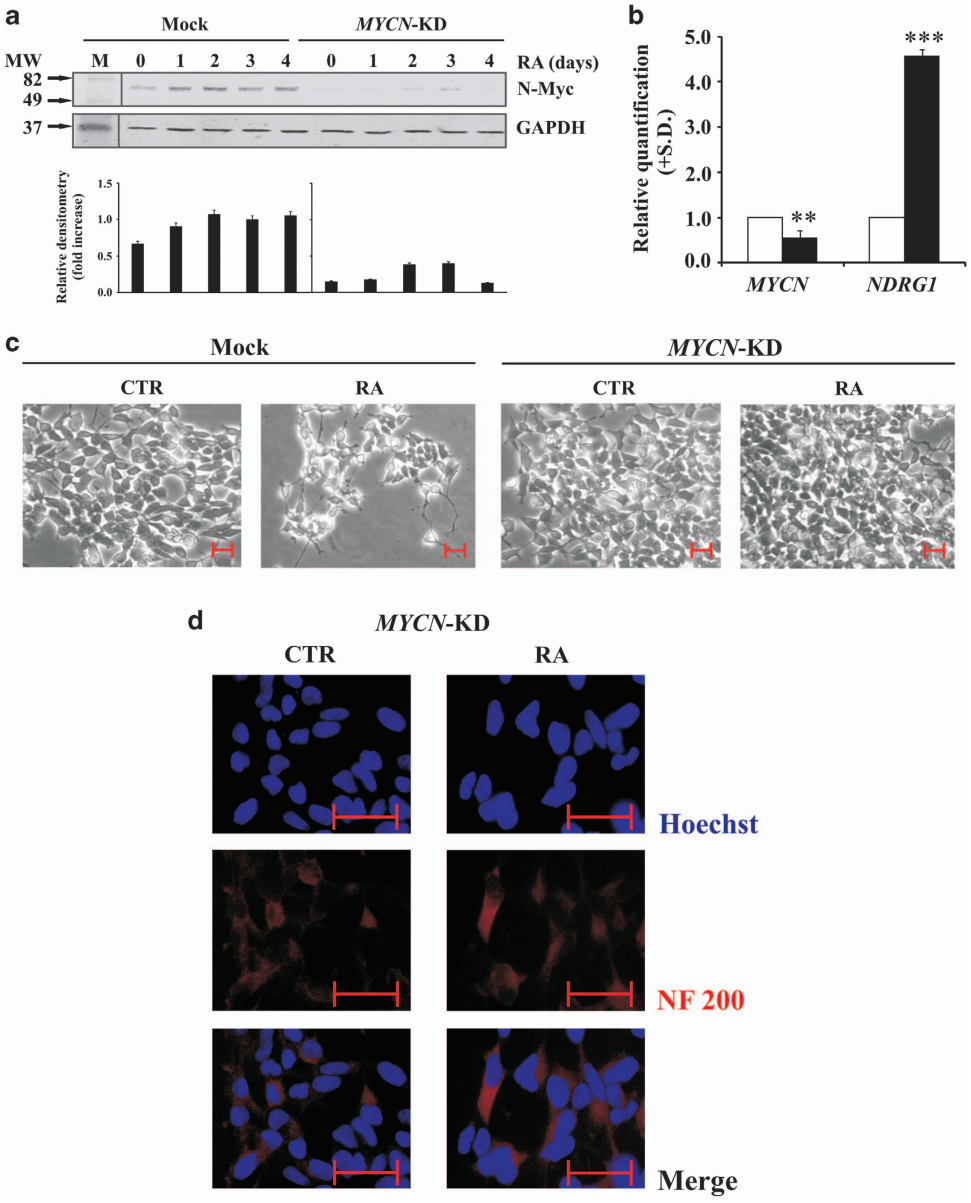

Figure 3 *MYCN* gene silencing in LAN-5 cells inhibits neurite outgrowth and NF200 expression after RA stimulus. (**a**) Upper panel, representative blots of the N-Myc protein in LAN-5 cells silenced for *MYCN* gene (*MYCN*-KD) or in control cells (Mock) untreated (0) or RA treated for 1, 2, 3, 4 and 5 days. M, molecular weight markers; MW, molecular weight. Lower panel, blots densitometry as analysed by ImageJ software. Values are averages + S.D. of three independent experiments with similar results. GAPDH expression was used to normalise protein loading. (**b**) The levels of the indicated mRNA in *MYCN*-KD LAN-5 cells (black) or in control cells (white). The data are reported as the level of mRNA relative to the respective control cells and are the mean + S.D. ($n = 3$). Statistical significance, $^{**}P \leq 0.01$; $^{***}P \leq 0.001$. (**c**) Inverted light microscope images in *MYCN*-KD LAN-5 cells or in Mock cells, untreated (CTR) or RA treated for 3 days. Scale bar, 50 μm. (**d**) Representative fluorescent images of *MYCN*-KD LAN-5 cells untreated (CTR) or RA treated for 3 days. Red, NF200 immunostaining; blue, Hoechst. Scale bar, 50 μm

development revealed changes in the expression of miR-20a, miR-9 and miR-92a. We found that these miRNAs were upregulated in *MYCN*-silenced LAN-5 cells (Figure 6a). In contrast, when *MYCN* was overexpressed in the SK-N-AS cells, the same miRNAs were downregulated (Figure 6b). In particular, the p53-family members have been reported to be regulated by these miRNAs. For this reason, we performed PCR array analysis of the p53 signalling pathway (Figure 6c). As expected, and consistent with the expression of miR-20a, miR-9 and miR-92a, the expression pattern observed in LAN-5 *MYCN*-KD cells was opposite to that in SK-N-AS *MYCN*+ cells with regard to genes known to be involved in cell death regulation. We found that pro-apoptotic *CASP9* and *BAI1* genes were upregulated in the *MYCN* overexpressing cells; whereas, the anti-apoptotic *BCL2* gene was downregulated in the same *MYCN* condition. By contrast, *CASP9* and *BAI1* were downregulated and *BCL2* was upregulated when *MYCN* was silenced. As well as, genes known to be involved in the activation of apoptotic programme such as *E2F1, E2F3, GADD45A* and *FOXO3* were upregulated in *MYCN*-amplified and downregulated in *MYCN*-silenced cells, respectively. In addition, despite an

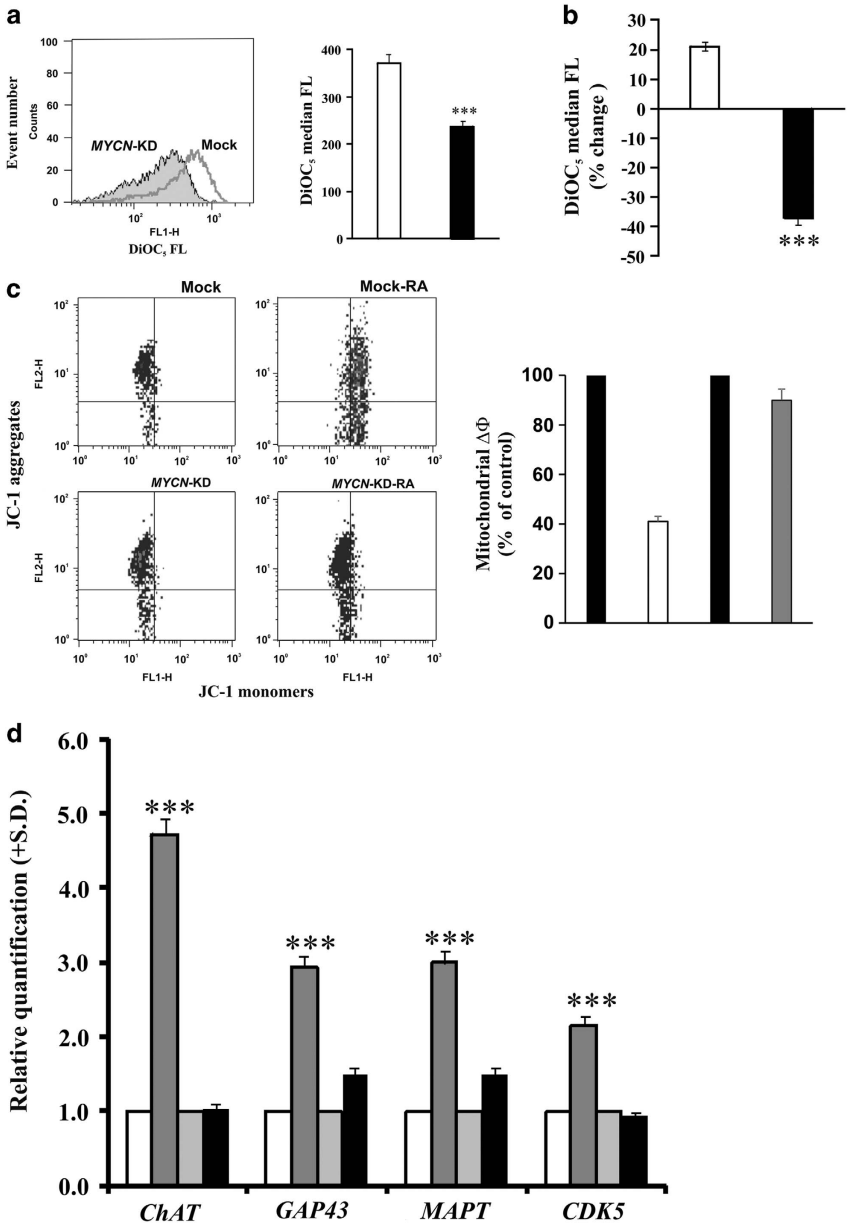

Figure 4 *MYCN* gene silencing produces a depolarisation of the plasma membrane and inhibits the RA-induced upregulation of differentiation markers. (**a**) Left, FACS analysis of the $DiOC_5$ fluorescence distribution in *MYCN*-KD LAN-5 cells (full histogram) or in Mock control cells (empty histogram). Right, median values of the $DiOC_5$ fluorescence distributions in *MYCN*-KD LAN-5 cells (black) or in Mock control cells (white). The experiment was repeated three times showing similar results. (**b**) The percent variation of the median values of the $DiOC_5$ fluorescence distributions in *MYCN*-KD LAN-5 cells (black) or in Mock control cells (white) after RA treatment. The experiment was repeated three times showing similar results. (**c**) Mitochondrial membrane potential analysed by JC-1 staining in Mock control LAN-5 untreated (Mock) and RA-treated (Mock-RA) cells compared with *MYCN*-KD LAN-5 untreated (*MYCN*-KD) and RA-treated (*MYCN*-KD-RA) cells (left panel). In the right panel are shown the $\Delta\Phi$ values calculated on the FACS cytograms following the formula described in Materials and Methods section. Data are reported as percent of control and are average of at least three separate experiments. Bars represent standard deviation. (**d**) The levels of the indicated mRNA in *MYCN*-KD LAN-5 cells untreated (light grey) or RA treated for 3 days (black) and in Mock control cells untreated (white) or RA treated for 3 days (dark grey). The data are reported as the level of mRNA relative to the respective untreated cells and are the mean + S.D. ($n = 3$). Statistical significance, $^{***}P \leq 0.001$

analysis of validated miRNA targets using miRWalk database reported miR-20a, miR-9 and miR-92a target *TP53, TP73* and *TP63* mRNAs, the PCR array analysis did not reveal any modulation of *TP53* mRNA levels (data not shown); whereas an upregulation of both *TP73* (about sevenfold) and *TP63* (more than twofold) was observed in *MYCN*-overexpressing cells (Figure 6c).

Inhibition of miR-20a, miR-9 and miR-92a in the wild-type SK-N-AS cells restores apoptosis and their differentiation ability. We inhibited miR-20a, miR-9 and miR-92a in *MYCN*-non-amplified SK-N-AS cells avoiding any possible interference by *MYCN* (Figure 7a).

The pro-apoptotic genes (*CASP9, FOXO3, E2F1, E2F3, TP73*) were upregulated by miRNAs inhibition after both 24 and 48 h.

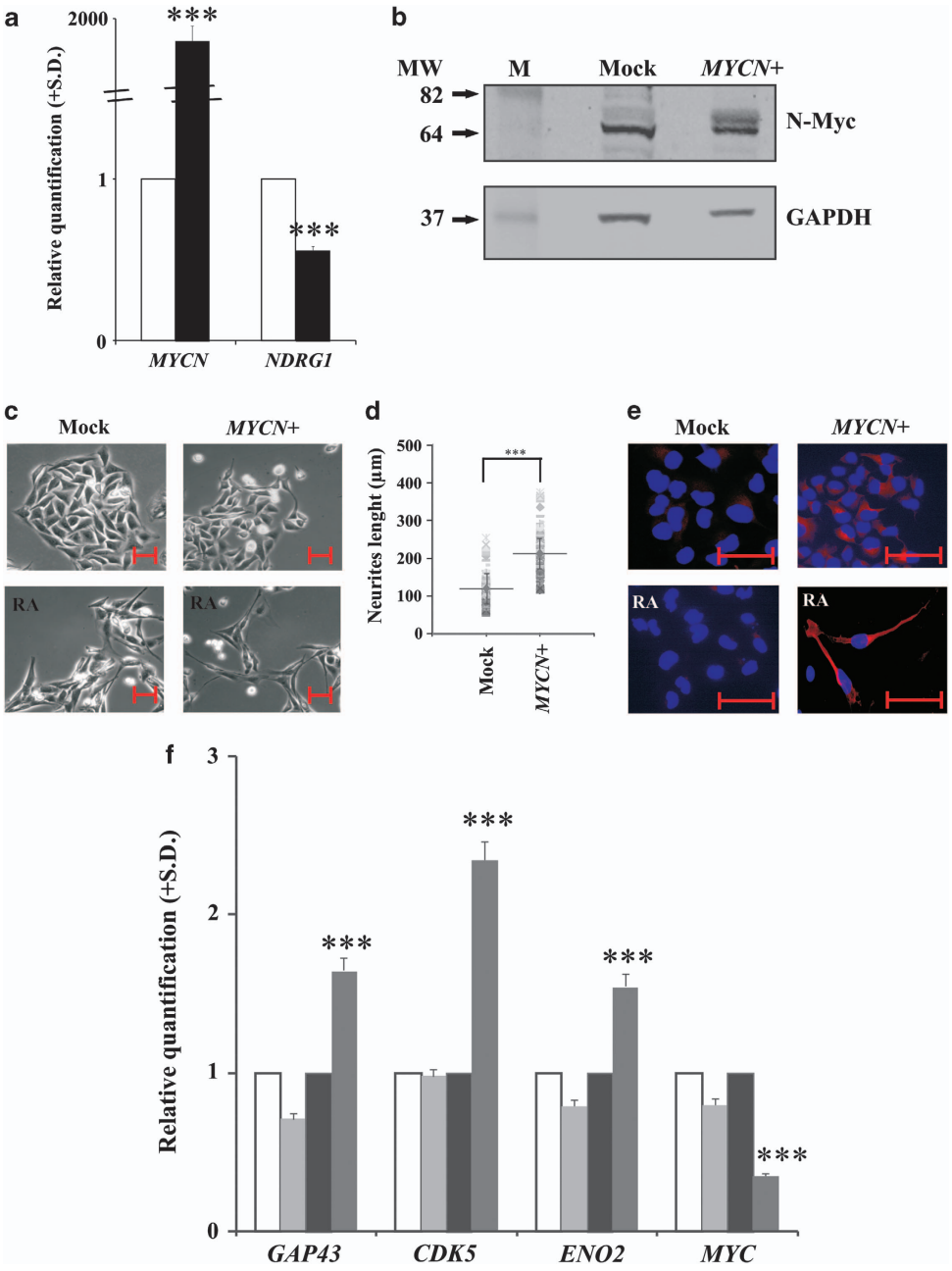

Figure 5 *MYCN* overexpression in the SK-N-AS cells restores their ability to differentiate after RA. (**a**) The levels of the indicated mRNA in SK-N-AS Mock (white) and SK-N-AS *MYCN*+ (black) cells. The data are reported as the level of mRNA relative to the respective Mock cells and are the mean + S.D. ($n = 3$). Statistical significance, ***$P \leq 0.001$. (**b**) Representative blots of the N-Myc protein in SK-N-AS Mock and SK-N-AS *MYCN*+ cells. GAPDH expression was used to normalise protein loading. The experiment was repeated three times showing similar results. M, molecular weight markers; MW, molecular weight. (**c**) Inverted light microscope images of SK-N-AS Mock and SK-N-AS *MYCN*+ untreated or RA treated for 3 days. Scale bar, 50 μm. (**d**) Distribution of the neurite outgrowth length as measured in SK-N-AS Mock and SK-N-AS *MYCN*+ treated with RA for 3 days. Statistical significance, ***$P \leq 0.001$. (**e**) Representative fluorescent images of SK-N-AS Mock and SK-N-AS *MYCN*+ untreated or RA treated for 3 days. Red, NF200 immunostaining; blue, Hoechst. Scale bar, 50 μm. (**f**) The levels of the indicated mRNA in SK-N-AS Mock and SK-N-AS *MYCN*+ untreated (white or black, respectively) or RA treated for 3 days (light grey or dark grey, respectively). The data are reported as the level of mRNA relative to the respective control cells and are the mean + S.D. ($n = 3$). Statistical significance, ***$P \leq 0.001$

By contrast, *TP63* was not upregulated suggesting no correlation between miR-20a, miR-9 and miR-92a and *TP63* expression (Figure 7b). Interestingly, RA was able to activate apoptosis after miRNAs inhibition in SK-N-AS cells (Figure 7c). Whereas control cells did not present any significant induction of apoptosis by RA treatment (Figure 7c).

Differentiation markers were upregulated after the inhibition of the three miRNAs at both 24 and 48 h in the presence of RA induction (Figure 7d). As expected, *MYC* was downregulated in differentiating cells.

In Figure 8a, we summarised our data presenting a hypothetical mechanism by which *MYCN* could trigger the

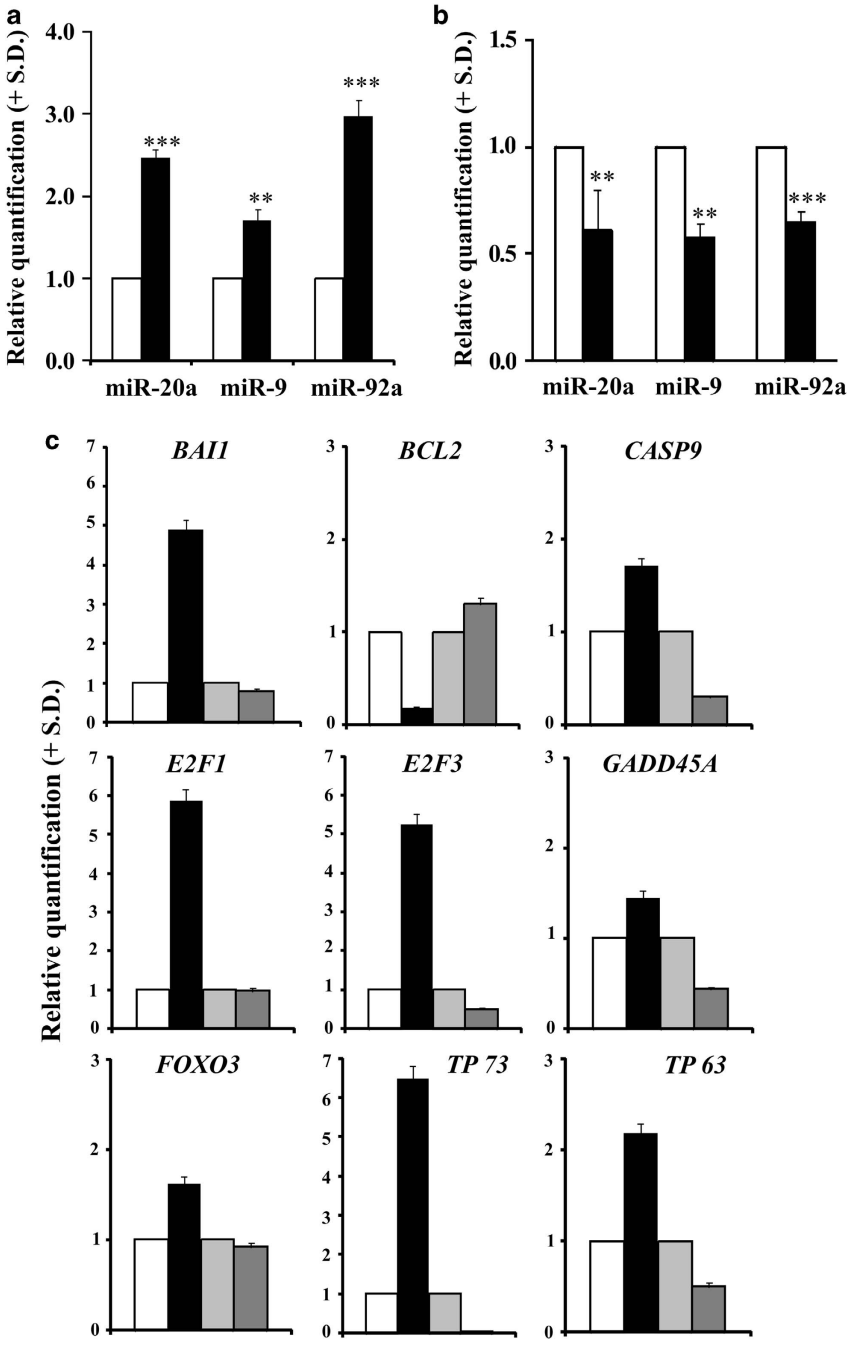

Figure 6 miRNAs are inversely regulated in *MYCN*-silenced and *MYCN*-upregulated neuroblastoma cells, and its expression is associated to a different modulation of apoptosis-related genes. (**a**) The levels of the indicated hsa-miR in *MYCN*-KD LAN-5 cells (black) or in Mock control cells (white). The data are reported as the level of miRNA relative to the respective untreated cells and are the mean + S.D. ($n = 3$). Statistical significance, $^{**}P \leq 0.01$, $^{***}P \leq 0.001$. (**b**) The levels of the indicated hsa-miR in SK-N-AS *MYCN*+ cells (black) or in Mock control cells (white). The data are reported as the level of miRNA relative to the respective untreated cells and are the mean + S.D. ($n = 3$). Statistical significance, $^{**}P \leq 0.01$; $^{***}P \leq 0.001$. (**c**) The levels of the indicated mRNA in SK-N-AS Mock (white), SK-N-AS *MYCN*+ (black), LAN-5 Mock (light grey) and LAN-5 *MYCN*-KD (dark grey). The data are reported as the level of mRNA relative to the respective control cells and are the mean + S.D. ($n = 3$)

onset of differentiation programme in neuroblastoma cells. To further validate this hypothesis, we analysed the expression kinetics of miRNAs and apoptotic genes presented in the model (Figure 8b, middle and lower panels). To make data reading easier, we reported the kinetics of *MYCN* gene (Figure 8a, upper panel; see also Figure 2b). As *MYCN* gene is upregulated during RA treatment, the three miRNAs are downregulated and consequently their targets are upregulated.

Discussion

Several studies of *MYC*- and *MYCN*-knockout mice have revealed that embryos of these mice could not survive until

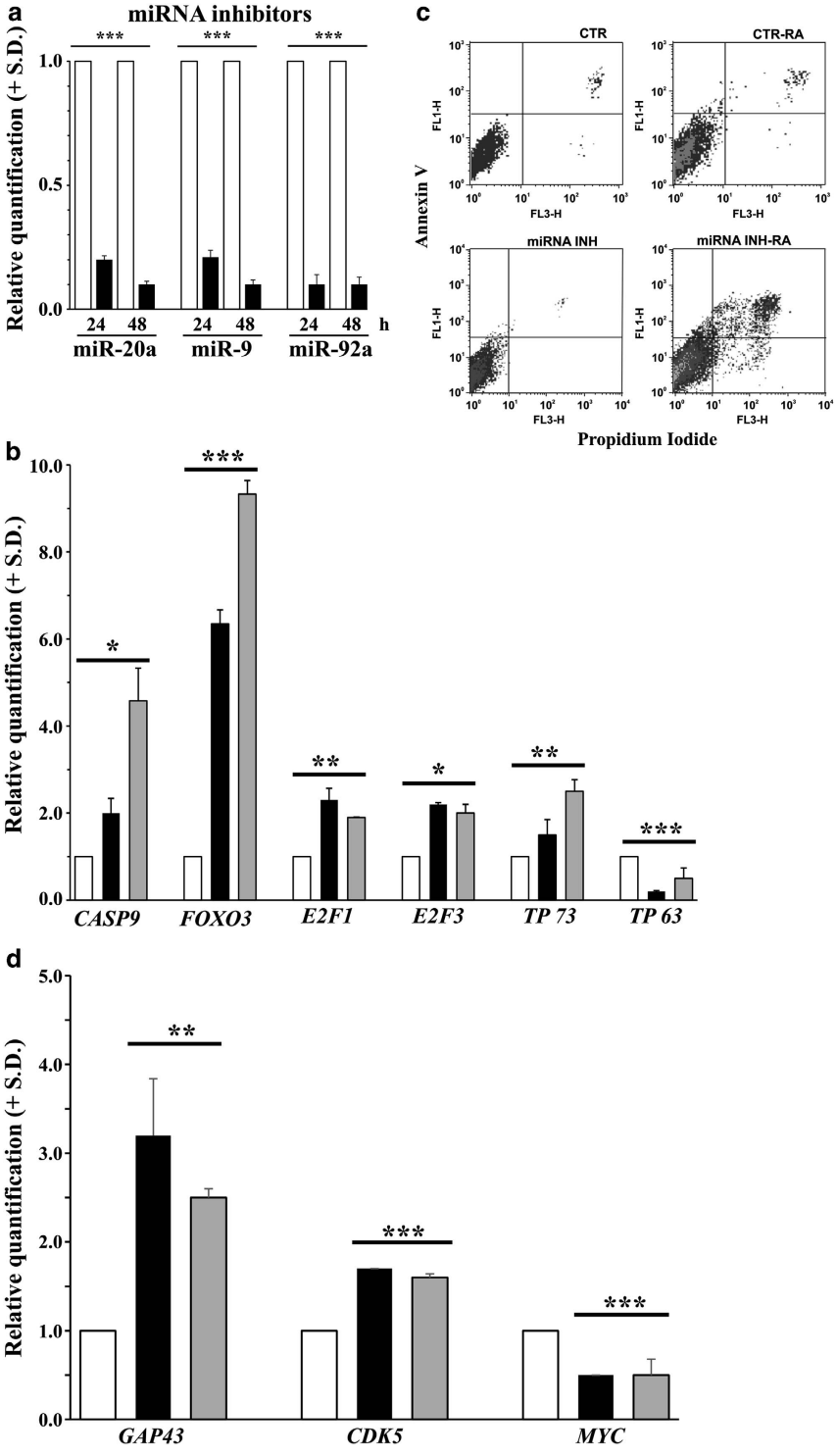

Figure 7 miR-20a, miR-9 and miR-92a inhibitions in wild-type SK-N-AS cells lead to apoptotic death induction and expression of differentiation-related genes. (**a**) The levels of the indicated miRNAs in inhibitor negative control (white) and miRNA inhibitor (black) cells at 24 and 48 h after transfection. The data are reported as the level of miRNAs relative to the respective miRNAs negative control cells and are the mean + S.D. ($n = 3$). Statistical significance, $^{***}P \leq 0.001$. (**b**) The levels of the indicated mRNA in inhibitor negative control (white), miRNA inhibitors at 24 h (black) and miRNA inhibitors at 48 h (grey). The data are reported as the level of mRNA relative to the respective miRNA negative control cells and are the mean + S.D. ($n = 3$). Statistical significance, $^{*}P \leq 0.05$; $^{**}P \leq 0.01$; $^{***}P \leq 0.001$. (**c**) FACS analysis of the Annexin V fluorescence distribution in inhibitor negative control untreated (CTR) and RA-treated (CTR-RA) cells and miRNA inhibitors untreated (miRNA-INH) and RA-treated (miRNA-INH-RA) at 48 h after transfection. The experiment was repeated three times showing similar results. (**d**) The levels of the indicated mRNA in inhibitor negative control (white), miRNA inhibitors at 24 h (black) and at 48 h (grey) after transfection. The data are reported in RA-treated condition. The data are the mean + S.D. ($n = 3$). Statistical significance, $^{**}P \leq 0.01$; $^{***}P \leq 0.001$

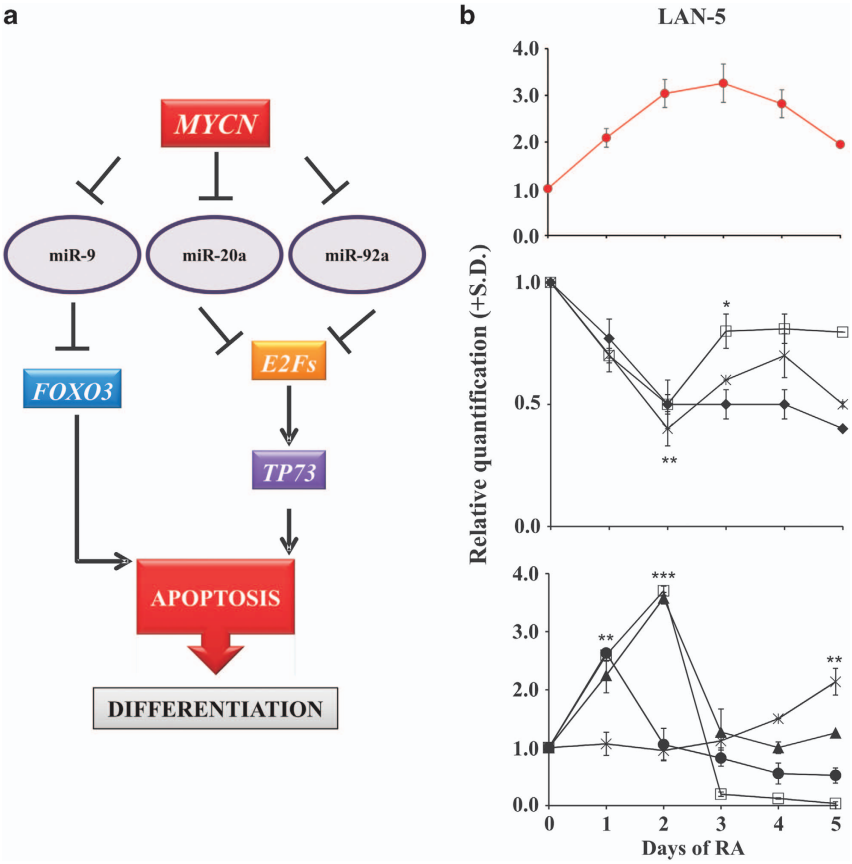

Figure 8 Model of the hypothetical role of *MYCN* during the early phases of neuroblastoma differentiation. (**a**) *MYCN* overexpression inhibits miR-9, miR-20a and miR-92a. We hypothesise that this inhibition allows targets of these miRNAs (*E2F* genes, *TP73* and *FOXO3*) to be upregulated and in turn to activate apoptosis in those cells not committed to differentiate but still proliferating. In contrast, *MYCN* downregulation allows the overexpression of miR-9, miR-20a and miR-92a, preventing the upregulation of apoptosis-related genes, thus inhibiting apoptosis and subsequent differentiation. (**b**) Upper panel, the levels of *MYCN* gene in LAN-5 cells untreated (0) or RA-treated for 1, 2, 3, 4 and 5 days. Middle panel, the levels of miR-20a (diamond), miR-9 (open square) and miR-92a (star). Lower panel, the levels of *E2F1* (closed circle), *E2F3* (open square), *FOXO3* (triangle), *TP73* (star). The data are reported as the level of mRNA relative to the respective untreated cells and are the mean + S.D. ($n = 3$). Statistical significance, $^{*}P \leq 0.05$; $^{**}P \leq 0.01$; $^{***}P \leq 0.001$

gestation,[11,14,16,23,24] suggesting that the *MYC* family genes are required for normal development at the beginning of organogenesis. In particular, Knoepfler *et al.*[24] showed that N-Myc has an important role in complete nervous system development. In fact, loss of N-Myc function during embryogenesis interrupts the ability of neural progenitors to expand, differentiate and populate the brain, causing neurological dysfunction after birth. Unlike c-Myc, which is expressed in all proliferating cells, N-Myc expression is more restricted. Appropriate spatial and temporal expression of N-Myc are important for normal embryonic development.[25] Accordingly, we show that upregulation of the *MYCN* gene is restricted to the early stages of differentiation induction in mouse cortical embryonic neural progenitor cells. In addition, as expected, *MYC* gene expression decreased during differentiation progress. These data suggest that the *MYCN* gene might have a critical role in the activation of neuronal differentiation. Nevertheless, as also reported by others,[19,26,27] differentiation completion was later associated with a decrease in *MYCN* expression. It is likely that the N-Myc protein, as a transcription factor, is necessary at the onset of neuronal differentiation to establish the expression of a set of genes essential for subsequent phases.

To examine the role of N-Myc in the neuronal differentiation programme, we used the human neuroblastoma cell line LAN-5, which show *MYCN* gene amplification.[28] The LAN-5 cell line, similar to many others neuroblastoma cell lines, maintains the ability to differentiate *in vitro* in the presence of specific stimuli, such as RA.[28,29] In fact, our results confirm that LAN-5 cells treated with RA form neurites; express the neuronal marker NF200, an intermediate filament that provides structural stability to the axon; and show the induction of a series of neuronal molecular markers. In agreement with previous papers,[27,30] *GAP43* and *MAPT* were upregulated in differentiated LAN-5 cells; in addition, *ChAT* and *SLC18A* appeared to have increased expression after differentiation induction in the LAN-5 cell line, which is normally committed to cholinergic differentiation.[2] As expected, successful development is associated with cell proliferation inhibition, demonstrated by cell cycle analysis performed using various approaches.

In addition to what has been observed previously,[19,26,27] we found peak *MYCN* expression during the first days of RA-induced differentiation in LAN-5 cells. We demonstrated the functionality of the increased N-Myc protein through expression analysis of the N-Myc target *NDRG1*, which decreased as expected.[20]

Furthermore, differentiation was inhibited by *MYCN* silencing in the same model; this was indicated by the failure of neurite outgrowth, the decrease in known neuronal molecular markers and the loss of NF200 expression during differentiation. In addition, the plasma membrane of the *MYCN*-KD LAN-5 cells depolarised and was no longer able to hyperpolarise in response to differentiation stimuli. Plasma membrane polarisation is a parameter known to be essential for differentiated neuronal cells.[31]

In addition, when *MYCN* is overexpressed in cells with a poor differentiation capacity, developmental processes are restored. This pattern was observed in SK-N-AS *MYCN*+ cells, in which neurite outgrowth occurred, and the expression of NF200 and known molecular neuronal markers increased after RA treatment.

These data, taken together, demonstrate that N-Myc protein expression is required to activate the differentiation processes in neuroblastoma cells.

To explore the mechanisms by which N-Myc could trigger differentiation in neuroblastoma cells, we studied the expression levels of miR20a, miR-9 and miR-92a, which have been reported to be involved in differentiation processes and to be modulated by *MYCN*.[32,33] Through the up- or downregulation of the *MYCN* gene, we observed that all the three miRNAs were decreased or increased, respectively. Consistently, the inverse relationship between these miRNAs and the cell differentiation status suggests that their downregulation is needed for differentiation triggering. In fact, according to the miRWalk database, two of the validated targets of these miRNAs are the RA receptor genes *RARA* and *RARG*.[34,35] The upregulation of miR-92a following *MYCN* silencing and its downregulation by RA treatment are in agreement with Chen and Stallings,[36] who showed that the expression of different miRNAs correlates with neuroblastoma prognosis, differentiation and apoptosis, also in response to RA. Moreover, consistently with Haug *et al.,*[37] who found that miR-92 inhibits the secretion of the tumour suppressor gene *DKK3* in neuroblastoma, our data demonstrated the downregulation of miR-92a in cells with a restored ability to differentiate, characteristic of a less malignant phenotype. Our findings are also supported by the data of Jee *et al.,*[38] which showed that inhibition of miR-20a expression induces definitive motor neuron survival and neurogenesis. Consistent with results of Yoo *et al*.,[39] showing that miR-9 is repressed in neural proliferating progenitors and is sequentially re-expressed in post-mitotic neurons, is the modulation of miR-9 we observed in LAN-5 cells during the RA kinetics (see Figure 8b, middle panel).

In agreement with O' Donnell *et al.*[40] and Coller *et al*.,[41] we demonstrated that miR-20a negatively regulates the *E2F* factor genes. The transactivating p73 isoforms are transcriptionally induced by E2F and contribute to E2F-mediated apoptosis.[42–44] Consistent with these data, upregulation of *TP73* and *E2F* was observed in *MYCN*+ cells and after miRNAs inhibition in SK-N-AS cells. Moreover, as expected, when *MYCN* was downregulated, and miR-20a and miR-92a were consequently upregulated, *E2F* and *TP73* were inhibited. The role of p73 in the induction of neuronal differentiation has been previously highlighted by De Laurenzi *et al*.,[45] who showed an increase in p73 protein levels after RA stimuli in murine neuroblastoma cells. In apparently disagreement with our data, they also showed reduced N-Myc protein levels after RA treatment as a marker of neuronal differentiation.[45] Indeed, they analysed N-Myc expression after 6 days of RA treatment, whereas, although our data demonstrated a peak in N-Myc protein expression between the second and the third day of differentiation induction, we also observed a subsequent decrease at day 5 of differentiation. It is likely that N-Myc, by downregulating miR-20a and miR-92a, produces the increase in *E2F*s gene expression, which in turn induces *TP73* transcription. Interestingly, RA treatment in LAN-5 cells confirmed the presence of a hierarchy between *E2F*s and *TP73,* which are overexpressed at day 1 and day 4 of RA treatment, respectively.

In addition, we found *FOXO3* upregulated in differentiating *MYCN*+ cells and in RA-treated LAN-5 cells. The human FOXOs transcription factor family regulates the expression of genes associated with multiple biological processes such as cell cycle arrest and apoptosis.[46] As demonstrated by Senyuk *et al*.,[47] miR-9 is able to bind directly to the 3′ UTR of *FOXO3*. In fact, when we silenced the *MYCN* gene in LAN-5 cells, an increase in miR-9 and a consequent decrease in *FOXO3* mRNA levels were obtained. These data are further demonstrated by the increase in *FOXO3* expression achieved after inhibiting miRNAs in SK-N-AS cells.

We reasoned that the miR-20a, miR-9 and miR-92a inhibition in *MYCN*+*,* as well as, in RA-treated LAN-5 cells and the subsequent pro-apoptotic genes increase could be a necessary step before differentiation programme. In fact, the inhibition of miR-20a, miR-9 and miR-92a in the *MYCN*-non-amplified SK-N-AS cells restored the ability of these cells to respond to RA treatment, as demonstrated by Annexin V assay and differentiation-related gene expression analysis.

Even though the overexpression of *MYCN* in SK-N-AS cells resulted in a downregulation of miR-92a and an upregulation of *TP63,* we did not observe an increase of *TP63* after inhibiting miR-92a. It is likely that other pathways downstream *MYCN* are involved in *TP63* regulation. More studies are needed to establish if *TP63* is directly or indirectly activated by N-Myc.

Therefore, we hypothesise that *MYCN* is necessary during the activation of neuroblastoma differentiation to induce apoptosis in cells that are not committed to differentiation but are still proliferating. Programmed cell death is a necessary physiological process and involves a large number of developing neurons during nervous system development[48] and in adult neurons.[49]

Materials and Methods

Cell line maintenance, differentiation and treatments. LAN-5 and SK-N-AS human neuroblastoma cell lines (both gifts of Dr. Doriana Fruci) were grown in RPMI-1640 medium (Gibco, Paisley, UK) supplemented with 10% FBS (Hyclone, South Logan, UT, USA), 2 mM L-glutamine, 10 U/l penicillin and 10 U/l streptomycin in a humidified incubator containing 5% CO_2 at 37 °C. LAN-5 cells contain amplified *MYCN*,[28] whereas SK-N-AS cells are *MYCN* single copy.[21]

Embryonic neural precursor cells (gift of Professor Stefano Biagioni and Dr. Emanuele Cacci) were cultured and differentiated as previously described.[50]

For differentiation experiments, LAN-5 cells were seeded at a density of 5×10^3 cells/cm^2. The following day, the cells were induced to differentiate with 10 μM retinoic acid (ATRA, designated RA throughout the paper; Sigma-Aldrich, St. Louis, MO, USA) in 'differentiation medium' composed of 50% fresh and 50% conditioned culture medium. The cells were fed after 3 days with differentiation medium containing fresh RA. RA was dissolved in dimethyl sulphoxide (Sigma-Aldrich) and stored as a stock solution at $-80\,^{\circ}$C. SK-N-AS cells were seeded at a density of 3.5×10^3 cells/cm^2. The following day, the cells were induced to differentiate by adding 1 μM RA in a 'differentiation medium' composed of RPMI + 1% FBS. Because of the light sensitivity of RA, all incubations were performed under subdued lighting. The dimethyl sulphoxide concentration in each experiment was always $\leq$0.01%, which was not toxic and did not induce differentiation.

A comparative western blot analysis has been conducted in the three cell lines employed in this work to evidence basal expression level of the main mentioned proteins (Supplementary Figure S1).

Neurite quantification. After RA treatment, the cells were viewed with a Leica DM IRB inverted phase contrast microscope at $\times$200 (Leica, Wetzlar, Germany). The cells were scored as differentiated if the length of the neurite extensions was at least twice the diameter of the cell body. The neurites were evaluated based on the percentage of cells bearing neurites as determined from the cell culture images, which facilitated tracing the individual neurites and eventual branch points. A total of $>$300 cells was examined in five randomly chosen fields in each treated and untreated sample. The projection images were semiautomatically traced with NIH ImageJ using the NeuronJ plugin. The total dendritic length of each individual neuron was analysed.

Western blot analyses. Cultured cells were washed twice with 1$\times$ PBS and then incubated for 1 min in urea buffer (8 M urea, 100 mM NaH_2PO_4 and 10 mM Tris pH 8), scraped, harvested and briefly sonicated. The proteins were subjected to SDS-polyacrylamide gel electrophoresis. The resolved proteins were blotted overnight onto nitrocellulose membranes, which then were blocked in 1$\times$ PBS containing 5% non-fat milk for at least 1 h. The blots were incubated with the following primary anti-human antibodies: rabbit polyclonal anti-N-Myc (C-19; Santa Cruz Biotechnology, Dallas, TX, USA); mouse monoclonal anti-GAP43 (GAP-7B10; Sigma-Aldrich); rabbit polyclonal anti-CDK5 (Cell Signaling Technology, Danvers, MA, USA); mouse monoclonal anti-cyclin A (C-19; Santa Cruz Biotechnology); rabbit polyclonal anti-p27^{kip1} (C-19; Santa Cruz Biotechnology); goat polyclonal anti-ChAT (Millipore, Billerica, MA, USA); mouse monoclonal anti-GAPDH (6C5; Millipore) and mouse monoclonal anti-HSP 72/73 (Ab1-W27; Oncogene Science Inc., Cambridge, MA, USA). The membranes were then incubated for 45 min with the appropriate secondary antibody: donkey anti-rabbit IRdye800 (LI-COR Biosciences, Lincoln, NE, USA); donkey anti-mouse IRdye800 (LI-COR) or donkey anti-goat IRdye800 (LI-COR). The membranes were then analysed with a Licor Odyssey Infrared Image System in the 800 nm channel. Blot scan resolution was 150 d.p.i.

Immunofluorescence. The cells were seeded on coverglass supports in complete medium and treated with RA for the indicated times. The cells were fixed with 4% (w/v) paraformaldehyde and permeabilised in PBS containing 0.1% Triton-X 100. NF200 was detected using an anti-NF200 monoclonal antibody (N52; Sigma-Aldrich). Alexa Fluor 594 goat anti-mouse antibody (Molecular Probes, Paisley, UK) was used as a secondary antibody. The antibodies were diluted in PBS. Cell nuclei were stained with 1 mg/ml DAPI or Hoechst 33342 in PBS for 5 min. Finally, the cells were washed in PBS and briefly rinsed in ddH_2O, and the coverglass slips were mounted in ProLong Gold anti-Fade Reagent (Molecular Probes). Images were acquired with an Olympus BX51 fluorescence microscope and analysed with I.A.S. software (Delta Sistemi, Legnano (VR), Italy). The brightness and contrast of the acquired images were adjusted, and the figures were generated using Adobe Photoshop 7.0.

Total RNA preparation. The cells were seeded in complete medium and harvested after the different treatments; total RNA was isolated using a Total RNA purification kit (Norgen Biotek, Thorold, ON, Canada). RNA quantity was determined by absorbance at 260 nm using a NanoDrop UV-VIS spectrophotometer (Thermo Fisher Scientific, Wilmington, DE, USA). The quality and integrity of each sample were confirmed using a BioAnalyzer 2100 (RNA 6000 Nanokit; Agilent, Santa Clara, CA, USA); samples with an RNA Integrity Number index lower than 8.0 were discarded.

Real-time RT-PCR analysis. RNA was reverse-transcribed with a High-Capacity cDNA Reverse Transcription Kit (Applied Biosystem, Paisley, UK) according to the manufacturer's instructions. Equal amounts of cDNA were then subjected to real-time PCR analysis with an Applied Biosystems 7900HT thermal cycler, using the SensiMix SYBR Kit (Bioline, London, UK) and specific primers, each at a concentration of 200 nM.: *GAPDH* (unigene Hs.544577) F: 5′-AG CCACATCGCTCAGACA-3′ and R: 5′-GCCCAATACGACCAAATCC-3′; *TBP* (Hs.590872) F: 5′-GAACATCATGGATCAGAACAACA and R: 5′-ATAGGGA TTCCGGGAGTCAT-3′; *MAPT* (Hs.101174) F: 5′-ACCACAGCCACCTTCTCCT and R: 5′-CAGCCATCCTGGTTCAAAGT-3′; *MYCN* (Hs.25960) F: 5′-CCACAA GGCCCTCAGTACC-3′ and R: 5′-TCCTCTTCATCATCTTCATCATCT-3′; *GAP43* (Hs.134974) F: 5′-GAGGATGCTGCTGCCAAG-3′ and R: 5′-GGCACTTTCCTT AGGTTTGGT-3′; *ChAT* (Hs.302002) F: 5′-CAGCCCTGATGCCTTCAT-3′ and R: 5′-CAGTCTTCGATGGAGCCTGT-3′; *SLC18A3* (Hs.654374) F: 5′-CCAGCC ACTCCTCAACCTT-3′ and R: 5′-GATATGGAACGGGTCACAGG-3′ and R: 5′-CC TTGAACACAGTTCCGTAGG-3′; *ENO2* (Hs.511915) F: 5′-ACTTTGTCAGGGACT ATCCTGTG-3′ and R: 5′-TCCCTACATTGGCTGTGAACT-3′; *CDK5* (Hs.647078) F: 5′-GCGATGCAGAAATACGAGAA-3′ and R: 5′-CCTTGAACACAGTTCCG TAGG-3′; *Mycn* (Mm.16469) F: 5′-CCTCCGGAGAGGATACCTTG-3′ and R: 5′-T CTCTACGGTGACCACATCG-3′; *Myc* (Mm. 2444) F: 5′-CCTAGTGCTGCATGAG GAGA-3′ and R: 5′-TCTTCCTCATCTTCTTGCTCTTC-3′; *Cdk5* (Mm.298798) F: 5′-TGGACCCTGAGATTGTGAAGT-3′ and R: 5′-GACAGAATCCCAGGCCTTT C-3′. Each experiment was performed in triplicate. The expression data were normalised using the Ct values of *GAPDH* and *TBP*.

To validate mRNA levels of genes identified by PCR array, we reverse-transcribed RNA with a High-Capacity cDNA Reverse Transcription Kit (Applied Biosystem) according to the manufacturer's instructions. Equal amounts of cDNA were then subjected to real-time PCR analysis with an Applied Biosystems 7900HT thermal cycler, using the 2$\times$ RT^2 SYBR Green/ROX qPCR Master Mix (Qiagen, Hilden, Germany) and specific primers, each at a concentration of 400 nM: *E2F1* (PPH00136G; Hs.654393); *E2F3* (PPH00917F; Hs.269408); *CASP9* (PPH00353B; Hs.329502); *FOXO3* (PPH00807A; Hs.220950); *TP63* (PPH01032F; Hs.137569); *TP73* (PPH00725A; Hs.697294).

miRNA assays. Equal amounts of RNA were reverse transcribed with the TaqMan MicroRNA Reverse Transcription Kit (Applied Biosystem), according to the manufacturer's instructions, with a custom 1$\times$ RT primer pool (hsa-miR-20a ID 000580; hsa-miR-9 ID 000583; hsa-miR-92a ID 000431). Real-time PCR analysis was performed with an Applied Biosystem 7900HT thermal cycler using 20$\times$ Individual TaqMan MicroRNA Assays.

miRNA inhibition. SK-N-AS cells were seeded at a density of 5×10^4 cells/cm^2. After 24 h, cells were transfected overnight in the presence of 10% FBS, both with mirVana miRNA inhibitors and mirVana miRNA inhibitor Negative Control. Lipofectamine RNAiMAX Reagent (Life Technologies, Paisley, UK) was used as transfection reagent according to manufacturer's instructions. We transfected hsa-miR-92a (MH10916, Ambion, Paisley, UK), hsa-miR20a (MH10057, Ambion) and hsa-miR9 (MH10022, Ambion) all together setting a concentration of approximately 10 nM each, in order to obtain the final concentration of 30 nM. The mirVana miRNA inhibitor Negative Control was used to the final concentration of 30 nM. After transfection cells were treated with RA (see Cell line maintenance, differentiation and treatments). Samples were harvested at 24 and 48 h to perform mRNA expression analysis and at 48 h to detect apoptosis.

PCR array. RNA was reverse transcribed with a High-Capacity cDNA Reverse Transcription Kit (Applied Biosystem) according to the manufacturer's instructions. Equal amounts of cDNA were then subjected to real-time PCR analysis with a Bio-Rad iQ5 thermal cycler. Each sample was mixed with 2$\times$ RT^2 SYBR Green/ROX qPCR Master Mix (Qiagen) and added to each 96-well plate of Human p53 Signaling Pathway PCR Array (PAHS-027A; Qiagen), according to the manufacturer's instructions.

Cell cycle analysis. Cell cycle analysis was performed by pulse-chase BrdU (Sigma-Aldrich) incorporation and propidium iodide (PI) DNA staining. For BrdU

incorporation, a pulse of 10 μM BrdU was added to the cell culture during the last 30 min before harvesting. Cells were fixed in ethanol 70% at + 4 °C for at least 1 h, and then processed as previously described. Primary anti-BrdU (BD Biosciences Italia, Buccinasco (MI), Italy) and secondary FITC-conjugated F(ab′)2 rabbit anti-mouse IgG (DAKO, Glostrup, Denmark) antibodies were used to detect the BrdU. Finally, after washing in PBS/BSA 0.5%, cells were stained with a solution containing 5 μg/ml PI and 75 KU/ml RNase overnight in dark. For PI staining, cells fixed in ethanol 70% for at least 1 h were stained in a solution containing 50 μg/ml PI and 75 KU/ml RNase for at least 30 min in the dark. In each case, 20 000 events per sample were acquired by using a FACScan cytofluorimeter and the CellQuest BD software. BrdU-positive cells represent the fraction of the cell population synthesising DNA. The percentages of the cells in the different cell cycle compartments were estimated on linear PI histograms by using the MODFIT software (Verity, Topsham, ME, USA).

Apoptosis detection. Apoptosis was detected in the specific conditions by using Annexin V assay, mitochondrial membrane potential measurement and estimation of sub-G1 fraction. Description of these methods have been detailed in previous papers.[51,52]

***MYCN* silencing.** Proliferating LAN-5 cells were transfected with a plasmid (pcDNA6.2-GW/EmGFP-miR-*MYCN*) targeting *MYCN* mRNA and a non-silencing plasmid (pcDNA6.2-GW/EmGFP-miR-Neg) with no homology to mammalian genes, using Lipofectamine2000 (Life Technologies) according to the manufacturer's instructions. We used 2 μg of plasmid. After transfection, the cells were selected with blasticidin for 2 weeks before performing experiments.

***MYCN* overexpression.** Proliferating SK-N-AS cells were transfected with a plasmid carrying the *MYCN* construct driven by the CMV promoter or a BlueScript control vector using Lipofectamine2000 (Life Technologies) according to the manufacturer's instructions. We used 2 μg of DNA per sample. At 24 h after the transfection, the cells were induced to differentiate by exposure to RA for 3 days using a specific differentiation protocol (see above).

Plasma membrane potential analysis. LAN-5 plasma membrane potential was measured by flow cytometry using the voltage-sensitive fluorescent dye $DiOC_5$ (Molecular probes). The cells were harvested and washed once in PBS + 0.1 M glucose, and 1×10^6 cells were incubated in a solution containing 50 nM $DiOC_5$ at 37 °C for 15 min. The samples were then washed once in PBS + 0.1 M glucose and immediately assessed by flow cytometry. As a depolarised control, we used a sample post-incubated with the oxidative phosphorylation inhibitor 4-trifluoromethoxyphenylhydrazone; as a hyperpolarised control, we used a sample incubated with the potassium-specific transporter valinomycin. PI at a final concentration of 10 μg/ml was added to each sample immediately before the measurements to exclude non-viable cells from the analysis. A total of 10 000 events was acquired for each sample using a FACScan cytofluorimeter.

Statistical analysis. Statistical significance of differences between groups was tested by paired Student's *t*-test or, if there were more than two groups, by one-way ANOVA.

Conflict of Interest

The authors declare no conflict of interest.

Acknowledgements. We thank Dr. Carla Musa for her contribution to our Laboratory. Partially supported by a joint Grant CNR-EBRI 'Molecular and cellular mechanisms of brain plasticity' and by PNR-CNR Aging Program 2012-2014.

1. Brodeur GM. Neuroblastoma: biological insights into a clinical enigma. *Nat Rev Cancer* 2003; **3**: 203–216.
2. Hill DP, Robertson KA. Characterization of the cholinergic neuronal differentiation of the human neuroblastoma cell line LA-N-5 after treatment with retinoic acid. *Brain Res Dev Brain Res* 1997; **102**: 53–67.
3. Munoz J, Vendrell E, Aiza G, Nistal M, Pestana A, Peinado MA *et al.* Determination of genomic damage in neuroblastic tumors by arbitrarily primed PCR: MYCN amplification as a marker for genomic instability in neuroblastomas. *Neuropathology* 2006; **26**: 165–169.
4. Eilers M, Eisenman RN. Myc's broad reach. *Genes Dev* 2008; **22**: 2755–2766.
5. Westermark UK, Wilhelm M, Frenzel A, Henriksson MA. The MYCN oncogene and differentiation in neuroblastoma. *Semin Cancer Biol* 2011; **21**: 256–266.
6. Malynn BA, de Alboran IM, O'Hagan RC, Bronson R, Davidson L, DePinho RA *et al.* N-myc can functionally replace c-myc in murine development, cellular growth, and differentiation. *Genes Dev* 2000; **14**: 1390–1399.
7. Murphy DM, Buckley PG, Bryan K, Watters KM, Koster J, van SP *et al.* Dissection of the oncogenic MYCN transcriptional network reveals a large set of clinically relevant cell cycle genes as drivers of neuroblastoma tumorigenesis. *Mol Carcinog* 2011; **50**: 403–411.
8. Pelengaris S, Khan M, Evan G. c-MYC: more than just a matter of life and death. *Nat Rev Cancer* 2002; **2**: 764–776.
9. Hui AB, Lo KW, Yin XL, Poon WS, Ng HK. Detection of multiple gene amplifications in glioblastoma multiforme using array-based comparative genomic hybridization. *Lab Invest* 2001; **81**: 717–723.
10. Nau MM, Brooks Jr BJ, Carney DN, Gazdar AF, Battey JF, Sausville EA *et al.* Human small-cell lung cancers show amplification and expression of the N-myc gene. *Proc Natl Acad Sci USA* 1986; **83**: 1092–1096.
11. Charron J, Malynn BA, Fisher P, Stewart V, Jeannotte L, Goff SP *et al.* Embryonic lethality in mice homozygous for a targeted disruption of the N-myc gene. *Genes Dev* 1992; **6**: 2248–2257.
12. Moens CB, Auerbach AB, Conlon RA, Joyner AL, Rossant J. A targeted mutation reveals a role for N-myc in branching morphogenesis in the embryonic mouse lung. *Genes Dev* 1992; **6**: 691–704.
13. Moens CB, Stanton BR, Parada LF, Rossant J. Defects in heart and lung development in compound heterozygotes for two different targeted mutations at the N-myc locus. *Development* 1993; **119**: 485–499.
14. Sawai S, Shimono A, Hanaoka K, Kondoh H. Embryonic lethality resulting from disruption of both N-myc alleles in mouse zygotes. *New Biol* 1991; **3**: 861–869.
15. Sawai S, Shimono A, Wakamatsu Y, Palmes C, Hanaoka K, Kondoh H. Defects of embryonic organogenesis resulting from targeted disruption of the N-myc gene in the mouse. *Development* 1993; **117**: 1445–1455.
16. Stanton BR, Perkins AS, Tessarollo L, Sassoon DA, Parada LF. Loss of N-myc function results in embryonic lethality and failure of the epithelial component of the embryo to develop. *Genes Dev* 1992; **6**: 2235–2247.
17. Squire J, Goddard AD, Canton M, Becker A, Phillips RA, Gallie BL. Tumour induction by the retinoblastoma mutation is independent of N-myc expression. *Nature* 1986; **322**: 555–557.
18. Zimmerman KA, Yancopoulos GD, Collum RG, Smith RK, Kohl NE, Denis KA *et al.* Differential expression of myc family genes during murine development. *Nature* 1986; **319**: 780–783.
19. Thiele CJ, Deutsch LA, Israel MA. The expression of multiple proto-oncogenes is differentially regulated during retinoic acid induced maturation of human neuroblastoma cell lines. *Oncogene* 1988; **3**: 281–288.
20. Melotte V, Qu X, Ongenaert M, van CW, de Bruine AP, Baldwin HS *et al.* The N-myc downstream regulated gene (NDRG) family: diverse functions, multiple applications. *FASEB J* 2010; **24**: 4153–4166.
21. Suenaga Y, Kaneko Y, Matsumoto D, Hossain MS, Ozaki T, Nakagawara A. Positive auto-regulation of MYCN in human neuroblastoma. *Biochem Biophys Res Commun* 2009; **390**: 21–26.
22. Dweep H, Sticht C, Pandey P, Gretz N. miRWalk–database: prediction of possible miRNA binding sites by "walking" the genes of three genomes. *J Biomed Inform* 2011; **44**: 839–847.
23. Davis A, Bradley A. Mutation of N-myc in mice: what does the phenotype tell us? *Bioessays* 1993; **15**: 273–275.
24. Knoepfler PS, Cheng PF, Eisenman RN. N-myc is essential during neurogenesis for the rapid expansion of progenitor cell populations and the inhibition of neuronal differentiation. *Genes Dev* 2002; **16**: 2699–2712.
25. Strieder V, Lutz W. E2F proteins regulate MYCN expression in neuroblastomas. *J Biol Chem* 2003; **278**: 2983–2989.
26. Amatruda III TT, Sidell N, Ranyard J, Koeffler HP. Retinoic acid treatment of human neuroblastoma cells is associated with decreased N-myc expression. *Biochem Biophys Res Commun* 1985; **126**: 1189–1195.
27. Sidell N. Retinoic acid-induced growth inhibition and morphologic differentiation of human neuroblastoma cells *in vitro*. *J Natl Cancer Inst* 1982; **68**: 589–596.
28. Ribatti D, Raffaghello L, Pastorino F, Nico B, Brignole C, Vacca A *et al.* In vivo angiogenic activity of neuroblastoma correlates with MYCN oncogene overexpression. *Int J Cancer* 2002; **102**: 351–354.
29. Edsjo A, Nilsson H, Vandesompele J, Karlsson J, Pattyn F, Culp LA *et al.* Neuroblastoma cells with overexpressed MYCN retain their capacity to undergo neuronal differentiation. *Lab Invest* 2004; **84**: 406–417.
30. Pahlman S, Ruusala AI, Abrahamsson L, Mattsson ME, Esscher T. Retinoic acid-induced differentiation of cultured human neuroblastoma cells: a comparison with phorbolester-induced differentiation. *Cell Differ* 1984; **14**: 135–144.
31. Sundelacruz S, Levin M, Kaplan DL. Role of membrane potential in the regulation of cell proliferation and differentiation. *Stem Cell Rev* 2009; **5**: 231–246.

32. Schulte JH, Horn S, Otto T, Samans B, Heukamp LC, Eilers UC *et al.* MYCN regulates oncogenic MicroRNAs in neuroblastoma. *Int J Cancer* 2008; **122**: 699–704.
33. Stallings RL. MicroRNA involvement in the pathogenesis of neuroblastoma: potential for microRNA mediated therapeutics. *Curr Pharm Des* 2009; **15**: 456–462.
34. Li G, Luna C, Qiu J, Epstein DL, Gonzalez P. Alterations in microRNA expression in stress-induced cellular senescence. *Mech Ageing Dev* 2009; **130**: 731–741.
35. Liu DZ, Ander BP, Tian Y, Stamova B, Jickling GC, Davis RR *et al.* Integrated analysis of mRNA and microRNA expression in mature neurons, neural progenitor cells and neuroblastoma cells. *Gene* 2012; **495**: 120–127.
36. Chen Y, Stallings RL. Differential patterns of microRNA expression in neuroblastoma are correlated with prognosis, differentiation, and apoptosis. *Cancer Res* 2007; **67**: 976–983.
37. Haug BH, Henriksen JR, Buechner J, Geerts D, Tomte E, Kogner P *et al.* MYCN-regulated miRNA-92 inhibits secretion of the tumor suppressor DICKKOPF-3 (DKK3) in neuroblastoma. *Carcinogenesis* 2011; **32**: 1005–1012.
38. Jee MK, Jung JS, Im YB, Jung SJ, Kang SK. Silencing of miR20a is crucial for Ngn1-mediated neuroprotection in injured spinal cord. *Hum Gene Ther* 2012; **23**: 508–520.
39. Yoo AS, Staahl BT, Chen L, Crabtree GR. MicroRNA-mediated switching of chromatin-remodelling complexes in neural development. *Nature* 2009; **460**: 642–646.
40. O'Donnell KA, Wentzel EA, Zeller KI, Dang CV, Mendell JT. c-Myc-regulated microRNAs modulate E2F1 expression. *Nature* 2005; **435**: 839–843.
41. Coller HA, Forman JJ, Legesse-Miller A"Myc'ed messages": myc induces transcription of E2F1 while inhibiting its translation via a microRNA polycistron. *PLoS Genet* 2007; **3**: e146.
42. Irwin M, Marin MC, Phillips AC, Seelan RS, Smith DI, Liu W *et al.* Role for the p53 homologue p73 in E2F-1-induced apoptosis. *Nature* 2000; **407**: 645–648.
43. Stiewe T, Putzer BM. Role of the p53-homologue p73 in E2F1-induced apoptosis. *Nat. Genet* 2000; **26**: 464–469.
44. Zaika A, Irwin M, Sansome C, Moll UM. Oncogenes induce and activate endogenous p73 protein. *J Biol Chem* 2001; **276**: 11310–11316.
45. De L V, Raschella G, Barcaroli D, Annicchiarico-Petruzzelli M, Ranalli M, Catani MV *et al.* Induction of neuronal differentiation by p73 in a neuroblastoma cell line. *J Biol Chem* 2000; **275**: 15226–15231.
46. Eijkelenboom A, Burgering BM. FOXOs: signalling integrators for homeostasis maintenance. *Nat Rev Mol Cell Biol* 2013; **14**: 83–97.
47. Senyuk V, Zhang Y, Liu Y, Ming M, Premanand K, Zhou L *et al.* Critical role of miR-9 in myelopoiesis and EVI1-induced leukemogenesis. *Proc Natl Acad Sci USA* 2013; **110**: 5594–5599.
48. Oppenheim RW. Cell death during development of the nervous system. *Annu Rev Neurosci* 1991; **14**: 453–501.
49. Kim WR, Sun W. Programmed cell death during postnatal development of the rodent nervous system. *Dev Growth Differ* 2011; **53**: 225–235.
50. Cacci E, Ajmone-Cat MA, Anelli T, Biagioni S, Minghetti L. *In vitro* neuronal and glial differentiation from embryonic or adult neural precursor cells are differently affected by chronic or acute activation of microglia. *Glia* 2008; **56**: 412–425.
51. Gatti G, Maresca G, Natoli M, Florenzano F, Nicolin A, Felsani A *et al.* MYC prevents apoptosis and enhances endoreduplication induced by paclitaxel. *PLoS One* 2009; **4**: e5442.
52. Maresca G, Natoli M, Nardella M, Arisi I, Trisciuoglio D, Desideri M *et al.* LMNA knock-down affects differentiation and progression of human neuroblastoma cells. *PLoS One* 2012; **7**: e45513.

Supplementary Information accompanies this paper on Cell Death and Disease website (http://www.nature.com/cddis)